An Experimental Examination of Riprap Effects on Homogeneous Embankment Dams Overtopping Breach

Mahdi Ebrahimi[1], Mirali Mohammadi[2*], Sayed Mohammad Hadi Meshkati[3], Farhad Imanshoar[4]

1-PhD Student, Department of Civil Engineering (Water & Hydraulic Structures), Faculty of Engineering, Urmia University, Urmia, Iran.
2-Professor, Department of Civil Engineering (Water & Hydraulic Structures), Faculty of Engineering, Urmia University, Urmia, Iran.
3-Assistant Professor, Department of Hydraulics and Hydro-Environmental Engineering, Water Research Institute, Tehran, Iran.
4- PhD Graduate, Iranian Water Resources Management Company, Tehran, Iran.

* m.mohammadi@urmia.ac.ir

Abstract

The overtopping phenomenon is the most common cause of embankment dams' failure, and it includes a complicate process. In present research, a physical model of an earthfill dam covered by riprap was constructed, and its hydraulic outcomes were compared with a benchmark model through providing a three-scenario framework. The main results indicated that the breach process of physical models follows three stages including: initiation, development, and termination. Furthermore, the use of riprap has no significant effects on the peak flow discharge caused by the breach procedure. In the first scenario, without a filter layer, the breach process had the highest resemblance to the benchmark model. For the second scenario, by employing a composite system, the occurrence of 129% increase in the breach time and the longest duration of the end stage were recorded. For the third scenario, by employing a composite system at the downstream slope, 86% increase in breach time and no change in the terminal stage duration was observed. Besides, the mass of eroded material was calculated according to the achieved sedimentation pattern. In the second scenario, the maximum thickness of the sediment was measured; it proved that the transport influence of riprap at the downstream of laboratory channel. A relatively symmetrical sedimentation pattern was then observed. Moreover, more than 50% of riprap material was transported to the downstream. This paper comprises the simultaneous measurements of breach geometry, flow hydrograph, and ultimate sedimentation patterns may help researchers in this field of study.

Keywords: Breach geometry, Dam failure, Flow hydrograph, Physical model, Riprap, Sedimentation pattern.

1. Introduction

Overtopping is the passage of water flow over the dam crest, which causes the dam body erosion and its destruction. Also, it mainly happens due to the lack of spillway sufficient capacity to discharge the flood, reduction of the reservoir storage capacity due to the sediment accumulation, and settlement of the dam (Association of state dam safety officials, 2023). The experimental tests of overtopping phenomenon regarding the protection of slope is of remarkable subject. Overtopping is the most probable cause of an embankment dam failure (Committee on dam safety, 2019). Moreover, there is insufficient laboratory data to evaluate the hydraulic influences of a homogeneous embankment dam failure. In addition, the effects of rock riprap have rarely been surveyed in previous studies. Investigating the embankment dam breach under overtopping is a vital subject, especially in terms of financial and environmental consequences management. Furthermore, regarding the sediment transport caused by the embankment dams breach, after useful life of dam, or the requirements for dam removal, it should identify the manner of sediment transport and sediment accumulation. The most important goals in the laboratory study of the embankment dams breach are obtaining the breach geometry, flow hydrograph, and the sedimentation pattern, some of which have been considered in previous studies. Evaluating the breach process depends upon both dam geometry, geotechnical characteristics, and the flood properties entering the dam reservoir. The analysis of the mentioned phenomenon has been done so far through comparative, semi-physical, and physical models, none of which are as important as laboratory modeling. This is because of the lack of laboratory modeling, and considering many simplifications may affect the accuracy of the results. There are various methods to prevent the slope erosion from wave action and water current, such as rock riprap, concrete, asphalt, and plant cover. Meanwhile, the historical experiences have proved that the most effective way to prevent the erosion is riprap. Riprap is a layer of large and durable rock fragments placed on a slope to prevent erosion. Many of the limestones and some of the sandstones make excellent riprap. Also, it is better to implement the riprap on a filter (bedding) layer; because of maintaining the riprap stability and prevent the shell soil erosion (Engomoen et al., 2014). The aforementioned protection method is called composite system. There are two methods to perform riprap: the hand-placed riprap and the dumped riprap. Dumped riprap failed in 5% of the cases where it was used; failures were attributed to improper size of stones. Hand-placed riprap failed in 30% of the cases where it was used; failures were attributed to the lack of suitable interlocking. Hence, dumped riprap is the preferred type of slope protection. Riprap is not compacted but is dumped to interlock the angular fragments. The minimum thickness of riprap layer should be 1.5 times the stone fragments' average diameter; plus, the layer should be sufficient to contain the largest rock (USBR, 1987 and Engomoen et al., 2014). A breach geometry looks like a trapezoidal shape. The most important parameters of the breach are observed in Fig. 1.
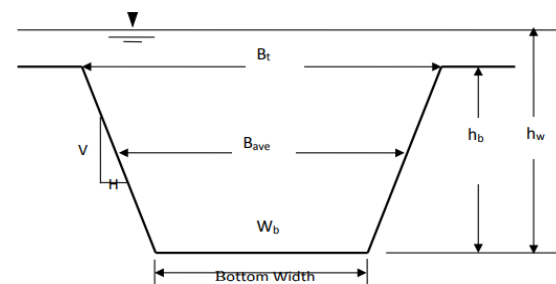
Fig. 1 Schematic shape of breach geometry (Brunner, 2016)

In Fig. 1, h_b is the breach section height, B_t is the breach section upper width, W_b is the breach section lower width, Bave is the breach section average width, V is the breach section vertical slope, H is the breach section horizontal slope, and hw is the overtopping water elevation. There are different stages to analyze the flow hydrograph. However, an important goal of its measurement is always to determine the peak flow discharge and its occurrence time. The sedimentation pattern involves the estimation of downstream topographical changes drawn by calculating the sedimentation thickness.

1.1. A Brief Literature Survey

Coleman et al. (2002) constructed homogeneous models in laboratory flumes. They found that an embankment dam erosion initially develops vertically and then laterally. In the IMPACT project (Morris and Hassan, 2005), large-scale and small-scale models were developed to gain

a deeper understanding of the breach process, data collection, and numerical model development. Pickert et al. (2011) conducted experiments and realized that coarser material has faster breach process. El-Ghorab et al. (2013) developed three homogeneous models with different heights and materials. The soil with higher erodibility showed larger breach geometry, shorter breach time, and higher maximum outflow. Al-Riffai (2014) focused on the geotechnical and hydraulic aspects of the breach mechanism by conducting experiments which had three phases. Hakimzadeh et al. (2014) utilized the genetic programming technics to propose a formula for peak discharge of homogeneous models. Its outcomes had a desirable agreement with observational values. Alhasan et al. (2015) analyzed the breach procedure of four dams which broke in the 2002 flood event at Czech Republic. Msadala (2016) developed new applied sediment transport equations for steep bed slopes to model homogeneous embankment dam's breach. Saberi (2016) developed the flow hydrograph resulting from the embankment dams breach with numerical methods. He concluded that if the primary breach channel is not dug on embankment dam crest, the maximum discharge will be higher, while the breach time will be shorter. Abdellatif Mohamed and El-Ghorab (2016) investigated small-scale physical models. Froehlich (2016) presented two non-linear mathematical models to predict the maximum discharge based on 41 events of breach. Sadeghi and Ahadiyan (2018) studied hydraulic breach process using four soil gradation. The results revealed that if the d_{50} increases, the groove outflow will increase. Further, the breach time will decrease. Kouzehgar et al. (2021) by developing homogeneous physical models, emphasized the important role of the breach average width in the outflow hydrograph, as well as the material gradation and compaction had remarkable role in the erosion rate. Ahadiyan et al. (2022) investigated the effects of riprapping on the failure mechanism of the levee. The results showed that the riprap cover had a significant impact on preventing the expansion of the levee breach, delaying the levee erosion, and increasing the levee failure time. As it is clear from the research background, although there are a few experimental studies on the breach process, they may not make a comprehensive view about all of hydraulic results. Also, there

is not experimental research regarding the simultaneous study of breach geometry, flow hydrograph, and sedimentation pattern after breach. Moreover, there is a huge gap about studying of the riprap effects on mentioned hydraulic results. In present research, three practical scenarios have been designed to investigate riprap influences on homogeneous physical models' breach: Scenario (I) the implementation of riprap on two slopes without filter layer; Scenario (II) the implementation of composite system on two slopes; Scenario (III) the implementation of composite system only on the downstream slope. Furthermore, the breach geometry, flow hydrograph, and sedimentation pattern results are compared with the benchmark model results.

2. Materials and Methods

2.1. Experimental Setup and Measurements

Physical modeling was performed at the hydraulics laboratory of the Iranian Water Research Institute (IWRI). To achieve the research objectives, a cement channel was constructed measuring one meter in width and with a slope of 2 in thousand. Three digital cameras placed at appropriate locations to evidence the breach geometry and measuring the downstream flow hydrograph. As the lake had a high-water volume, it was unnecessary to empty it to complete the breach process. Thus, the breach finishing time was recorded by analyzing the camera records in front of the upstream slope. To measure the flow hydrograph, a 90° V-notch weir was utilized at 5.5 m away from the physical model toe (Fig. 2). Equation 1 was used to calculate the flow hydrograph (in m³/s) through the 90° V-notch weir (Novak et al., 2017):

$$Q = \frac{8}{15} \times \sqrt{2g} \times C_d \times \tan\left(\frac{\theta}{2}\right) \times H^{2.5} \qquad (1)$$

In the equation above, C_d denotes the discharge coefficient, which is a function of the V-notch angle (θ), and H is the water level on the V-notch (in meters). Based on the preliminary experiments, the downstream sedimentation length was 4 meters. Sedimentation thickness was determined at 140 points by placing a cart on the channel using a laser meter (channel bed elevation difference before and after the sedimentation process). Then, the

sedimentation plan was drawn by Surfer software. The inlet flow to fill the upstream lake was 2.5 lit/s, while the lake volume at breach initiation was 4.3 m³. After the completion of each test, the recorded video was saved on the laboratory computer. Accordingly, Plot Digitizer software acquired the breach geometry and flow hydrograph data. Fig. 2 presents a schematic diagram for the experimental setup in present study.
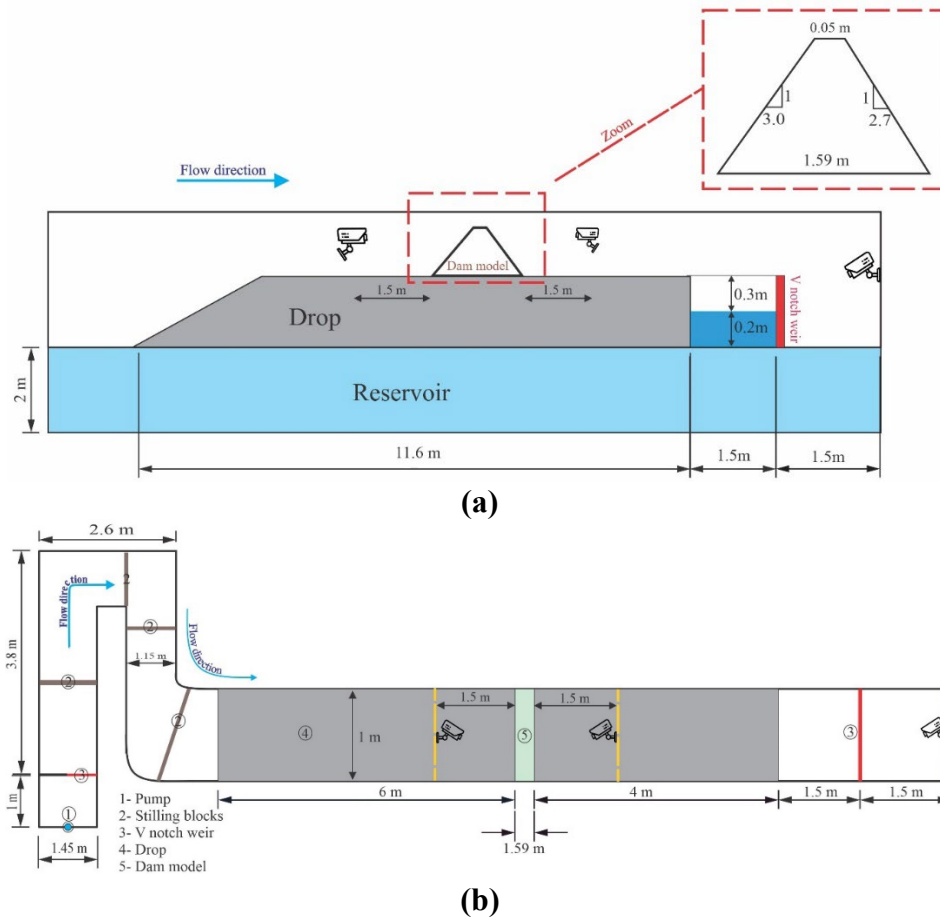

(a)

(b)

Fig. 2 Experimental setup rig: (a) side view and (b) plan view.

2.2. Construction procedure of physical models

Before starting the experiments, the sand and riprap samples were examined by the soil mechanics laboratory. The optimum moisture content was determined to be 9.2% (ASTM D422-63, 2002 and ASTM D1557, 2007), and internal friction angle parameter was found as 35 degrees with no cohesion (ASTM D3080, 2003). The models were constructed based on the design principles mentioned in reliable sources (USBR, 1987 and USACE, 2004). Each of the physical models was made in six layers (five layers with a thickness of five centimeters and one layer with a thickness of two centimeters). The compaction operation of shell material was done by falling flat hammers at optimal humidity percentage and continued to

the point where it was no longer possible to vary the volume. Equation 2 was used to calculate the compaction percentage (Υ_d is the dry specific weight). Table 1 reports the shell specifications. Before initiating the test, a rectangular groove measuring 10 cm in length and 2.5 cm in depth was dug in the crest middle to guide the breach process. After constructing each physical model, the riprap was dumped using angular and resistant limestones (its water absorption percentage and its relative density were determined 0.1% and 2.72 respectively by soil mechanics laboratory). Fig. 3 displays the gradation diagrams of the shell, riprap, and filter layer, which were determined by the soil mechanics laboratory.

$$R = \frac{\Upsilon_d}{\Upsilon_{dmax}} \times 100 \qquad (2)$$
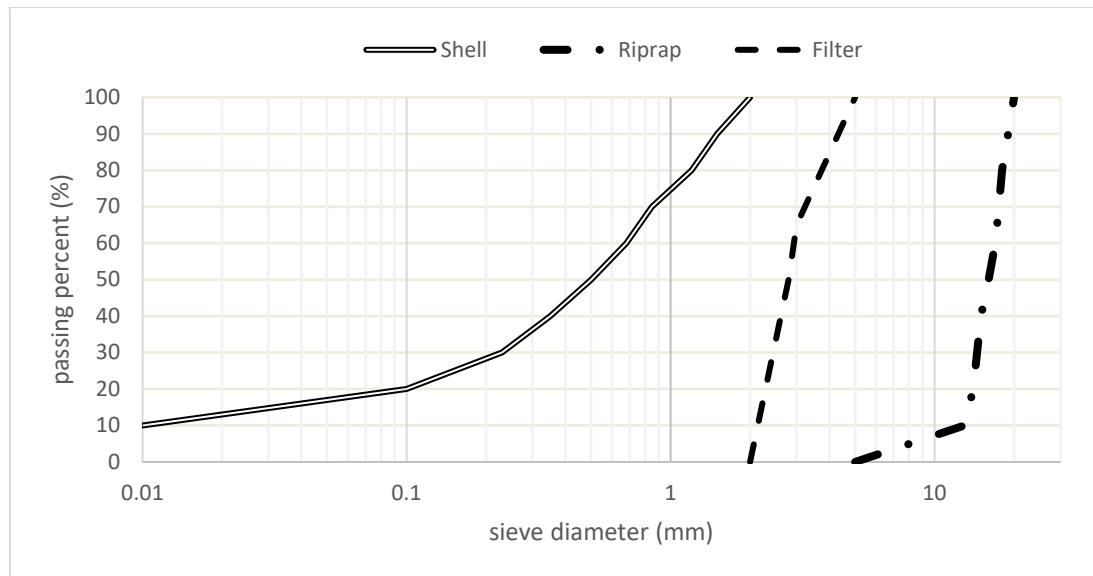
Fig. 3 Materials grain size distribution curves

Table 1. Shell properties

Height (cm)	Top width (cm)	Bottom width (cm)	Upslope (V:H)	Downslope (V:H)	Weight (kg)	Compaction percent
27	5	159	1:3	1:2.7	296	69

2.3. Experiments Program

This research presents the results of four types of experiments: The first test was the benchmark test (the common test for the homogeneous embankment dams physical modeling), which was repeated to ensure the results. The results of three scenarios were then compared with benchmark test, which are: Scenario (I) riprap was performed on two slopes; Scenario (II) a composite system (simultaneous performance of riprap and filter on two slopes) was done; Scenario (III) the composite system was performed only on downstream slope. The overtopping breach began as soon as the water entered the downstream slope. The upstream lake water level was 24.5 cm at the beginning of all tests. To ensure the minimum thicknesses of the riprap and the filter ($1.5D_{50}$), which were 25 mm for the riprap and 5 mm for the filter layer, the mass listed in Table 2 was utilized.

To determine the dry specific weight of the sediments caused by homogeneous models' breach, four random samples were taken from the accumulated bed sediment and placed in an oven for 24 hours to dry. The dry materials specific weight was obtained through dividing the dry sample mass by its volume. Based on the calculations, a figure of 1450 kg/m3 for the dry specific weight was chosen.

Table 2. Riprap and filter mass in different scenarios

Title	Riprap mass (kg)	Filter mass (kg)
Sc1	61	0
Sc2	61	25
Sc3	31	13

3. Results and Discussion

3.1. Benchmark Model Results

The breach geometry and flow hydrograph are drawn in the diagrams below (i.e., Figs. 4 & 5). According to the laboratory observations and graphs obtained based on the cameras analysis, the physical models breach process can be described in three important stages, specifically for the benchmark model (see Fig. 6).

3.1.1. The first stage: Breach initiation

The first stage begins when water enters the downstream slope. The breach process continues in a straight path along the primary groove in the crest. At this stage, the dimensions of the groove do not increase significantly. Since the weir measured the flow hydrograph at

5.5 m the physical model toe, there was a delay of 55 seconds for measuring the initial breach flow by the mentioned weir. The duration of initiation stage was calculated as 50 seconds based on the camera records in front of the downstream slope. Thus, the weir does not register the flow discharge thorough the initiation duration. According to the observations, most eroded sediment was located a part near the physical model toe.
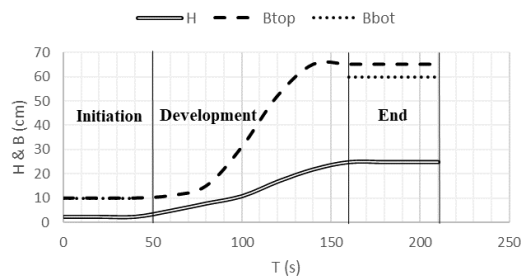

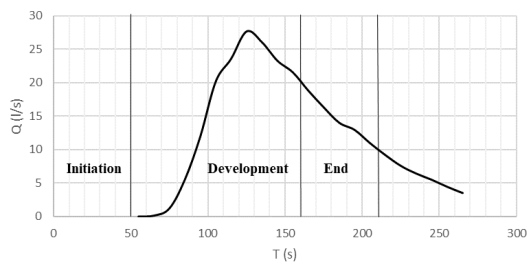**Fig. 4** The benchmark breach geometry variations

Fig. 5 The benchmark breach hydrograph

3.1.2. The second stage: Breach development

After the initiation phase, the breach process enters the development stage. The dimensions of the rectangular groove increase significantly, and the physical model breach section reaches its final value (the breach section height, the breach section upper width, and the breach section lower width reached 25 cm, 65 cm, and 60 cm, respectively). The numbers related to the breach section lower width could not be recorded in the development stage because of the state of water flow submergence, and thus were not drawn in the relevant diagrams. The greatest variations in breach geometry occurred in the development stage. In the flow hydrograph diagram, the rising limb and part of the falling limb (including the 27.7 lit/s peak discharge at 125 seconds after breach initiation) are related to the development stage. The development stage duration was 110 seconds. According to the observational results, the main part of the sedimentation pattern was formed in this stage.

3.1.3. The third stage: Breach end

At this stage, the breach section dimensions would not change significantly. Still, the interaction between the flow and the physical model upstream slope continued until the upstream slope deformation reached its final state (the remaining thickness of the physical model heel reached 6 cm). The final stage duration was 50 seconds. The final stage results
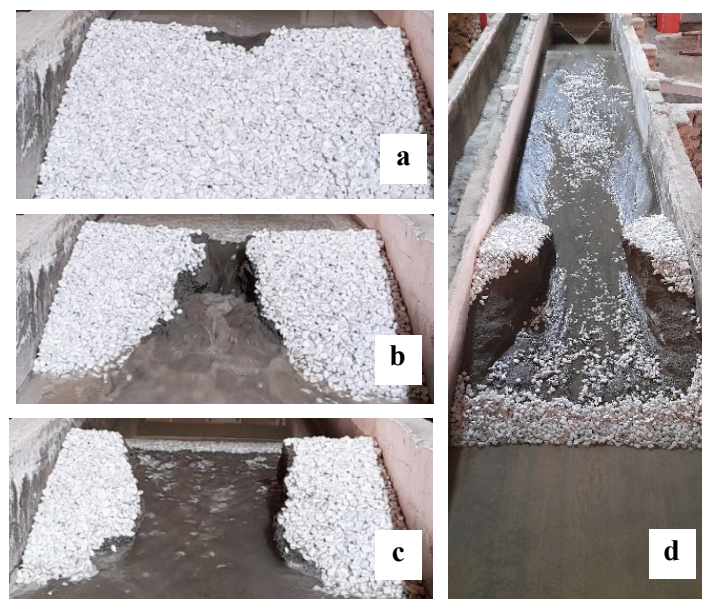

Fig. 6 Breach phases: (a) initiation, (b) development, (c) end and (d) final status.

also showed a noticeable reduction in the breach flow intensity and small changes in the sedimentation pattern. Moreover, the average slope of the breach section was measured at 84°.

3.2. Breach Geometries Comparison

In the graphs below, the breach geometry of the benchmark model has been compared with other scenarios (see Figs. 7- 9).

According to the mentioned diagrams, the final breach section heights were 25 cm in different tests. Also, the thickness of the remaining sediment was 2 cm in the final breach section. Thus, the difference in the final breach geometries will be related to the variations in the breach section widths. In the third scenario, the breach width increased approximately at 5 cm of the channel bed (Fig. 10). In different tests, the breach section slope was between 84

degrees and 89 degrees. The highest breach time belonged to the second scenario (129% longer than the benchmark test), followed by the third scenario, which had an 86% increase in comparison with the benchmark model. The first scenario breach process was very similar to the benchmark model, indicating the influence of neglecting the filter layer. In the second and third scenarios, the initiation stage duration was longer than the development and end stages. It can be related to the overtopping flow absorption by the filter layer, delaying the start of interaction between overtopping flow and the physical model shell. In the second scenario, the maximum duration of the end stage was recorded, and in the third scenario, the duration of the end stage was the same as the benchmark model, which proves riprap ignorance effects on the upstream slope. Table 3 compares the final figures of the breach geometries.
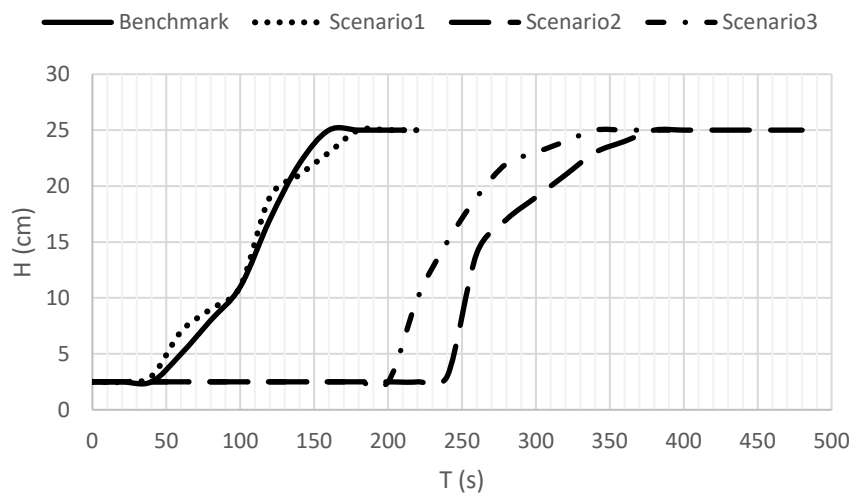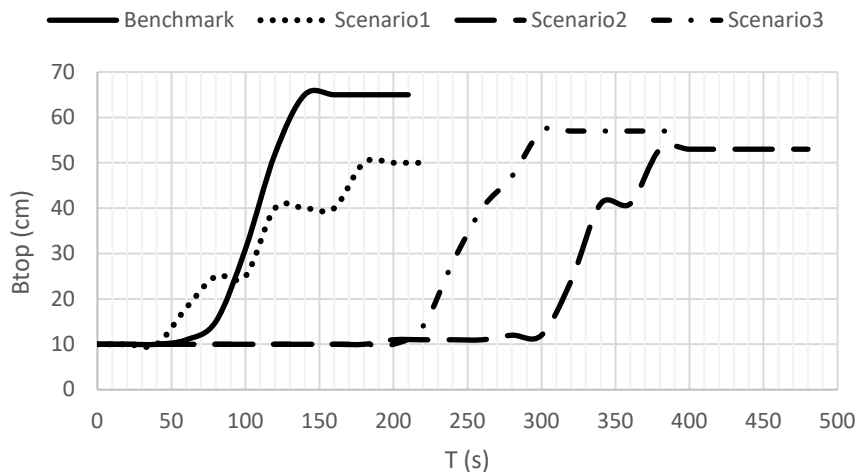

Fig. 7 A comparison of breach heights

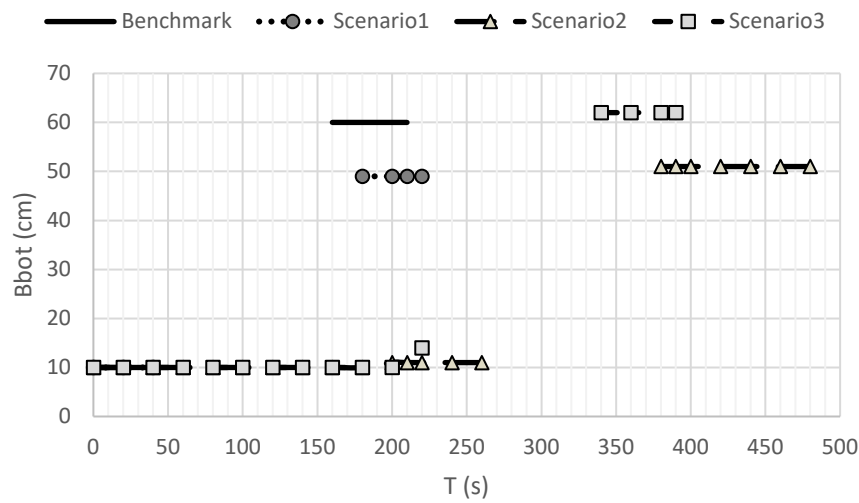**Fig. 8** A comparison of breach top widths

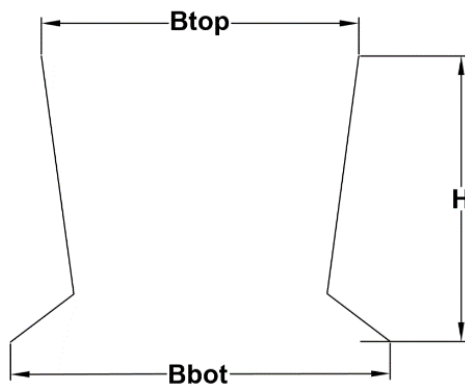**Fig. 9** A comparison of breach bottom widths

Fig. 10 The breach geometry in third scenario

3.3. Flow hydrographs comparison

The diagram below compares the benchmark test flow hydrograph and those of other scenarios (see Fig. 11). By analyzing the obtained results, slight changes in the peak discharge were observed in different scenarios. In the first scenario, the breach duration and peak outflow occurrence time had the least difference in comparison to the benchmark model. Besides, in the second scenario, they had the largest difference with the benchmark model. Table 3 reveals the comparison between the final numbers of breach hydrographs.
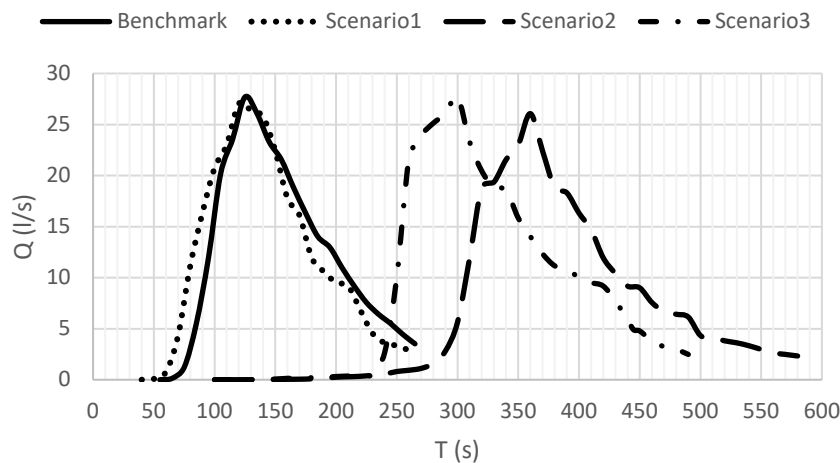

Fig. 11 A comparison of breach hydrographs

3.4. Sedimentation patterns comparison

Fig. 12 compares the sedimentation patterns of the benchmark model and other scenarios (the laboratory channel dimensions are in centimeters, and the scale numbers are in millimeters).

Table 3 Models breach geometry and flow hydrograph results

Subject	Breach time (s)	Height (cm)	Top width (cm)	Bottom width (cm)	Average side slope (degree)
Benchmark	210	25	65	60	84
Scenario 1	220	25	50	49	89
Scenario 2	480	25	53	51	88
Scenario 3	390	25	57	62	85
Subject	**Peak discharge (lit/s)**	**Peak flow time (s)**	**Initiation duration(s)**	**Development duration(s)**	**End duration(s)**
Benchmark	27.7	125	50	110	50
Scenario 1	27	120	50	130	40
Scenario 2	26	360	270	110	100
Scenario 3	27.7	300	220	120	50
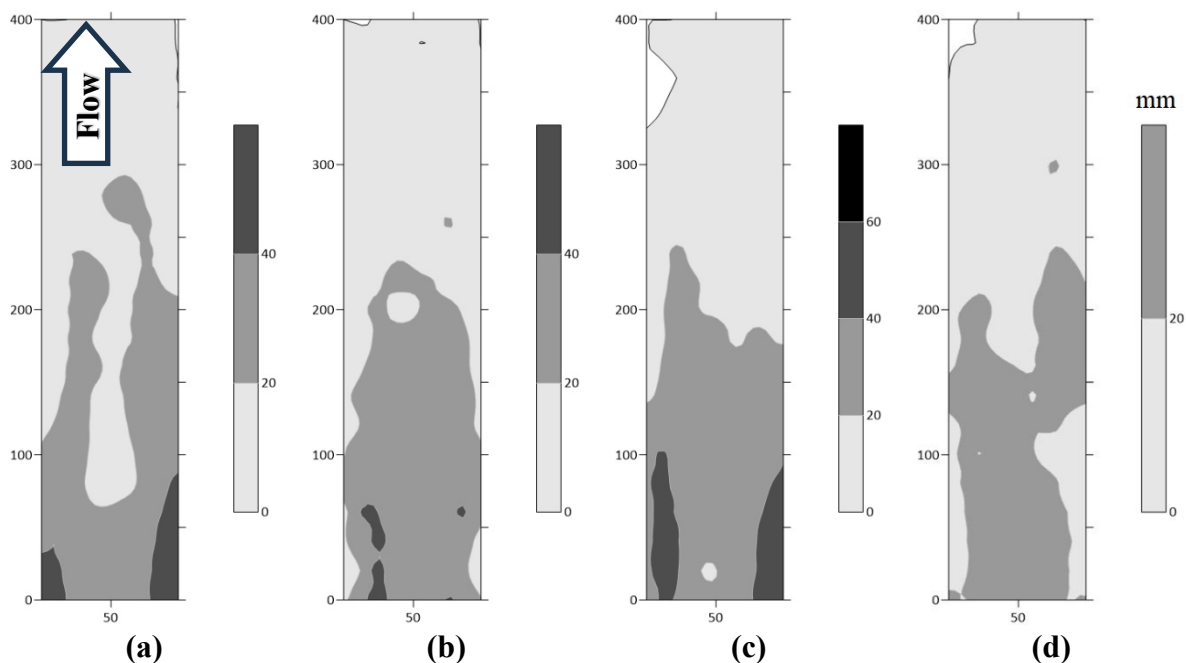
Fig. 12 A comparison of sedimentation patterns after dam failure in different scenarios: (a) benchmark, (b) scenario 1, (c) scenario 2 and (d) scenario 3

In Table 4, the numbers related to the average sediment thickness obtained by averaging from 140 points. Also, the eroded material volume was obtained by Surfer software. Moreover, the average sediment mass was obtained by multiplying the eroded material volume by sediment density. In addition, the mass of riprap transported downstream was measured with a scale. For the benchmark model, the average sediment thickness was calculated to be 18.2 mm. Besides, the eroded material volume was calculated to be $0.073 m^3$ and its corresponding mass would be 105.6 kg. Therefore, one of the practical results of the sedimentation pattern determination is calculating the volume and mass of eroded material. Based on Fig. 12, the sediment thickness diminished upon moving downstream. Due to the digging of the primary breach groove in the physical models crest middle, the breach geometry and the sedimentation pattern had a relatively symmetrical shape. The average sediment thickness was higher than the benchmark model in different scenarios. The highest thickness (22.6 mm) belonged to the second scenario, indicating the effects of implementation of the composite system on the upstream and downstream slopes. According to Table 4, more than 50% of riprap material has moved downstream. Also, according to the observations,

Table 4. Sedimentation pattern results

Subject	Average sedimentation thickness (mm)	Eroded material volume (m³)	Sediment mass (kg)	Riprap mass (kg)
Benchmark	18.2	0.073	105.6	
Scenario 1	20.1	0.08	116.6	39/61
Scenario 2	22.6	0.09	131.1	38/61
Scenario 3	19	0.076	110.2	16/31

the main part of riprap put at region of the channel bed middle part.

4. Conclusions

This paper reports an experimental examination of overtopping by establishing physical models including riprap on the dam side slopes with different scenarios. The main results of the research are presented as follows:

- The breach process of physical models generally includes three stages: initiation, development, and termination. The development stage involves the lateral development of the breach channel formed in the downstream slope until the breach geometry finalization.

- In the second and third scenarios, the duration of the start stage was longer than the other two stages. Also, in the second scenario, the duration of the end stage was longer than other tests, which proves the effectiveness of the filter layer implementation.

- In all the tests, the final height of the breach section was measured as 25 cm; thus, the difference in breach geometry was related to the difference in the upper and lower widths. Also, the final breach geometry had an almost trapezoidal shape.

- In the first scenario, in which the riprap was performed on the upstream and downstream slopes, the least difference was observed in the breach process and flow hydrograph in comparison to the benchmark model. Also, by comparing the flow hydrographs, the peak discharge did not significantly vary in different scenarios.

- The highest breach time belongs to the second scenario, followed by the third scenario, which increased by 129% and

86%, respectively, compared to the benchmark model. It indicates the effect of the filter layer implementation.

- Due to the digging of the primary groove in the crest middle, an almost symmetrical sedimentation pattern was observed. The maximum thickness of the downstream sedimentation, as well as its corresponding volume and mass, belongs to the second scenario. The effects of carrying the riprap downstream was visible in the average thickness of the sedimentation pattern. Further, more than 50% of the riprap material moved downstream. Considering the observations, most of the riprap was located at a region of the channel bed in mid part.

5. Notation

h_b	Schematic breach section height [m]
B_t	Schematic breach section upper width [m]
W_b	Schematic breach section lower width [m]
B_{ave}	Schematic average breach section width [m]
V	Schematic breach section vertical slope [-]
H	Schematic breach section horizontal slope [-]
h_w	Schematic overtopping water elevation [m]
H	Breach section height [cm]
B_{top}	Breach section upper width [cm]
B_{bot}	Breach section lower width [cm]
T	Time [s]
Q	Breach outflow (discharge) [lit/s]
C_d	Discharge coefficient [-]
H	Water level on the V-notch [m]
θ	V-notch angle [degree]
R	Compaction percentage [-]
Υ_d	Dry specific weight [kg/m³]
Υ_{dmax}	Maximum dry specific weight [kg/m³]

6. References

Abdellatif Mohamed, M.M. & El-Ghorab, E.A.S. (2016). Investigating scale effects on breach evolution of overtopped sand embankments. *Water Sci, 30*, 84-95.

Ahadiyan, J., Bahmanpouri, F., Adeli, A., Gualtieri, C. & Khoshkonesh, A. (2022). Riprap effect on hydraulic fracturing process of cohesive and non-cohesive protective levees. *Water Resour Manag*, *36,* 625-639.

Alhasan, Z., Jandora, J. & Ríha, J. (2015). Study of dam-break due to overtopping of four small dams in the Czech Republic. *Acta Universitatis Agriculturae et Silviculturae Mendelianae Brunensis*, *63*, 717-729.

Al-Riffai, M. (2014). Experimental study of breach mechanics in overtopped non-cohesive earthen embankments. PhD thesis, University of Ottawa, Ottawa, Canada.

Association of state dam safety officials (2023). Kentucky, USA. https://damsafety.org.

ASTM D422-63 (2002). Standard test method for particle size analysis of soils.

ASTM D1557 (2007). Standard test methods for laboratory compaction characteristics of soil using standard effort. West Conshohocken, PA, USA.

ASTM D3080 (2003). Standard test method for direct shear test of soils under consolidated drained conditions. Annual Book of ASTM Standards, Philadelphia 408, 1-7.

Brunner, G.W. (2016). HEC-RAS Reference Manual, version 5.0. Hydrologic Engineering Center, Institute for Water Resources, US Army Corps of Engineers, Davis, California.

Coleman, S.E., Andrews, D.P. & Webby, M.G. (2002). Overtopping breaching of non-cohesive homogeneous embankments. *J. Hydraul. Eng.*, *128*, 829-838.

Committee on dam safety (2019). ICOLD incident database bulletin 99 update: statistical analysis of dam failures. Technical report, international commission on large dams. https://www.icoldchile.cl/boletines/188.pdf

EL-Ghorab, E.A., Fahmy, A. & Fodda, M. (2013). Large scale physical model to investigate the mechanics of embankment erosion during overtopping flow. *Eng. Res. J.*, *36*, 287-302.

Engomoen, B., Witter, D.T., Knight, K. & Luebke, T.A. (2014). Design Standards No 13: Embankment Dams, USBR.

Froehlich, D.C. (2016). Predicting peak discharge from gradually breached embankment dam. *J. Hydrol. Eng.*, *21*, 04016041, http://dx.doi.org/ 10.1061/(ASCE)HE.1943-5584.0001424.

Hakimzadeh, H., Nourani, V. & Amini, A.B. (2014). Genetic programming simulation of dam breach hydrograph and peak outflow discharge. *J Hydrol Eng*, *19*, 757-768.

Kouzehgar, K., Hassanzadeh, Y., Eslamian, S., Yousefzadeh Fard, M. & Babaeian Amini, A. (2021). Physical modeling into outflow hydrographs and breach characteristics of homogeneous earthfill dams failure due to overtopping. *Journal of Mountain Science*, *18*, 462-481.

Morris, M. & Hassan, M. (2005). IMPACT: Investigation of extreme flood processes and uncertainty-a European research project. In: Defra Flood and Coastal Management Conference 2005, 5-7 July 2005, York, UK.

Msadala, V.P. (2016). Sediment transport dynamics in dam-break modelling. PhD thesis, Stellenbosch University, Stellenbosch, South Africa.

Novak, P., Moffat, A.I.B., Nalluri, C. & Narayanan, R. (2017). Hydraulic Structures. CRC Press.

Pickert, G., Weitbrecht, V. & Bieberstein, A. (2011). Breaching of overtopped river embankments controlled by apparent cohesion. *J. Hydraul. Res.*, *49*, 143-156.

Saberi, O. (2016). Embankment dam failure outflow hydrograph development. PhD Thesis, Graz University of Technology, Austria.

Sadeghi, E. & Ahadiyan, J. (2018). Hydraulically failure mechanism of non-cohesive homogeneous protective embankments by overtopping. *Journal of Irrigation Sciences and Engineering*, *41*, 115-131.

USACE (2004). General design and construction considerations for Earth and rockfill dams. US Army Corps of Engineers, Washington DC, USA.

USBR (1987). Design of small dams. Bureau of Reclamation, Water Resources Technical Publication.